Quantum Dots

DOI: 10.1002/anie.200906262

Water Splitting by Visible Light: A Nanophotocathode for Hydrogen Production**

Thomas Nann, Saad K. Ibrahim, Pei-Meng Woi, Shu Xu, Jan Ziegler, and Christopher J. Pickett**

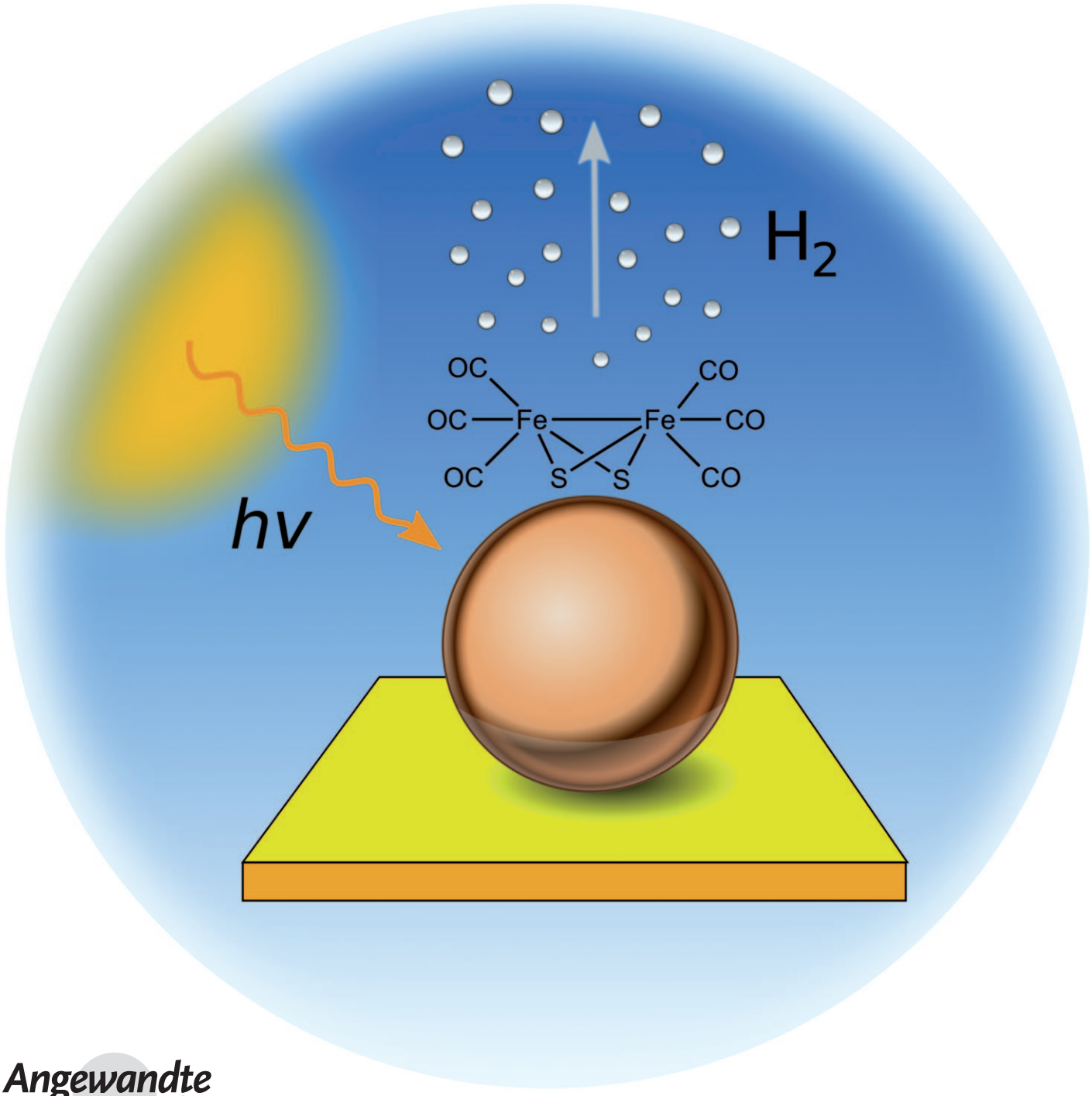

Efficient production of solar fuels is an imperative for meeting future fossil-fuel-free energy demands. Hydrogen that is derived from the splitting of water by solar energy is clearly attractive as a clean energy vector, and there have been many attempts to construct viable molecular and biomolecular devices for photohydrogen production.[1] A common approach in the construction of such devices is the utilization of tris(bipyridine)ruthenium, zinc porphyrin, or related molecular materials as photosensitizers in conjunction with a tethered or free electrocatalyst or enzymic system.[2–4] Apart from cost, such systems suffer from having limited lifetimes, which may be attributed at least in part to the intrinsic reactivity of the organic N-donor ligands in the radical anion form of the photoexcited state and photodegradation pathways.[5,6]

Herein we show that an inexpensive and environmentally benign inorganic light harvesting nanoarray can be combined with a low-cost electrocatalyst that contains abundant elements. This system provides a stable photoelectrochemical platform for hydrogen production. The device is constructed by first building-up a cross-linked indium phosphide (InP) nanocrystal array layer by layer and then incorporating an iron–sulfur electrocatalyst. Iron–sulfur carbonyl assemblies related to the subsite of [FeFe]-hydrogenase have been shown to electrocatalyze the reduction of protons to dihydrogen under dark conditions at potentials between −0.7 and −1.4 V versus the standard calomel electrode (SCE) in non-aqueous electrolytes.[7,8] Of these assemblies, we chose $[Fe_2S_2(CO)_6]$, which has sulfide bridges that are potentially capable of binding to indium as a catalyst for photoelectrochemical reduction of protons in a solid-state assembly, and a modest reduction potential of −0.90 V versus SCE. With this system, we were able to achieve a photoelectrochemical efficiency of more than 60%, which is a major breakthrough in this field.

First, we show that $[Fe_2S_2(CO)_6]$ can quench the luminescence of InP nanocrystals. Then, we show by Fourier-transform infrared spectroscopy (FTIR) that a three-dimensional array of InP nanocrystals and the subsite can be assembled on a supporting gold substrate. Thereafter, we show that this assembly supports a substantial photocurrent in an aqueous electrolyte, and finally that the InP-catalyst array produces hydrogen on the preparative scale and at a potential bias significantly positive of the dark equilibrium potential for proton reduction at pH 7.

[*] Prof. Dr. T. Nann, Dr. S. K. Ibrahim, P.-M. Woi, Dr. S. Xu, Dr. J. Ziegler, Prof. Dr. C. J. Pickett
Energy Materials Laboratory, School of Chemistry
University of East Anglia
Norwich NR4 7TJ (UK)
Fax: (+44) 1603-59-2003
E-mail: t.nann@uea.ac.uk
c.pickett@uea.ac.uk

[**] T.N. gratefully acknowledges receipt of a Royal Society Wolfson Merit Award. The work presented here was supported by the Engineering and Physical Sciences Research Council (EPSRC) and the German Federal Ministry for Education and Research (BMBF). P.-M.W. was supported by the University of Malaya, Kuala Lumpur, under the Fundamental Research Grant Scheme (FP086-2007C).

InP nanocrystals were prepared according to our previously published procedure as 5 nm particles with an emission band at 600 nm and a full width at half maximum (FWHM) of about 80 nm.[9,10] These nanocrystals were dispersed in toluene using hexadecylamine (HDA) and the zinc salts of long-chain fatty acids (stearic and undecanoic acid) as surface ligands. The fluorescence of InP nanoparticles in dispersion in toluene is slowly quenched in the presence of the simple hydrogenase subsite analogue, $[Fe_2S_2(CO)_6]$, under oxygen-free conditions. This quenching is indicative of the binding of the subsite to the InP photosensitizer. Figure 1 shows the

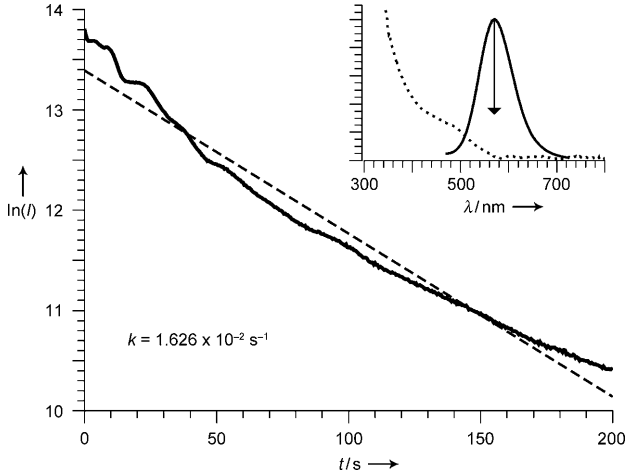

Figure 1. Luminescence quenching of InP quantum dots by $[Fe_2S_2(CO)_6]$ in toluene. The process follows roughly a first-order rate law with rate constant *k*. Inset: UV/Vis absorption and photoluminescence spectrum of InP quantum dots in cyclohexane.

temporal evolution of the photoluminescence intensity of the InP nanocrystals upon exposure to $[Fe_2S_2(CO)_6]$ in toluene. The response is consistent with the slow exchange of surface ligands with the subsite analogue. The photoluminescence of the quantum dots was completely quenched when the system was equilibrated and a sufficient concentration of the subsite analogue was present. Luminescence quenching may have been caused by charge transfer, non-radiative energy transfer, or introduction of defect states into the InP band structure by $[Fe_2S_2(CO)_6]$.

The nanocathode array was assembled by first modifying gold electrodes by adsorbing a monolayer of 1,4-benzenedithiol, which enabled the binding of a primary layer of the InP nanocrystals to the gold. Layer-by-layer buildup of the nanoparticle assembly was achieved by alternate exposure to the dithiol and the nanocrystal solutions. Finally, the $[Fe_2S_2(CO)_6]$ cluster was introduced onto/into the assembly by exposure of the modified electrode to a solution of $[Fe_2S_2(CO)_6]$ in toluene, followed by thorough rinsing with toluene. Figure 2 shows a representation of the modified gold electrode.

The presence of the $[Fe_2S_2(CO)_6]$ subsite absorbed within the assembly was confirmed by (diffuse) reflectance FTIR spectroscopy. Figure 3 shows the carbonyl stretching region for the parent complex in solution and that for the bonded

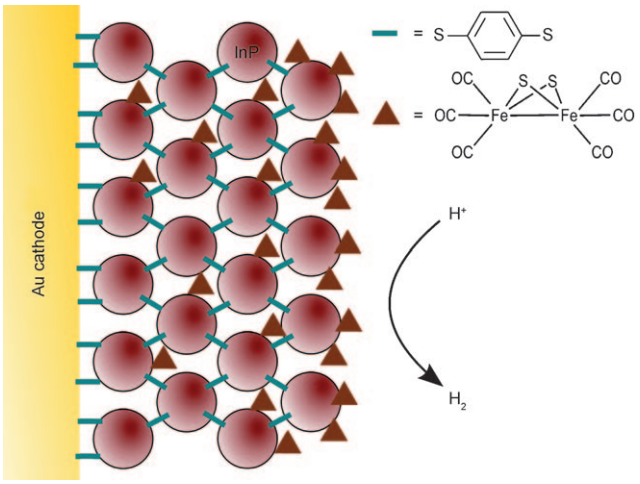

Figure 2. Cross-section of a InP nanocrystal-modified gold electrode with adsorbed/intercalated $[Fe_2S_2(CO)_6]$ subsite analogue.

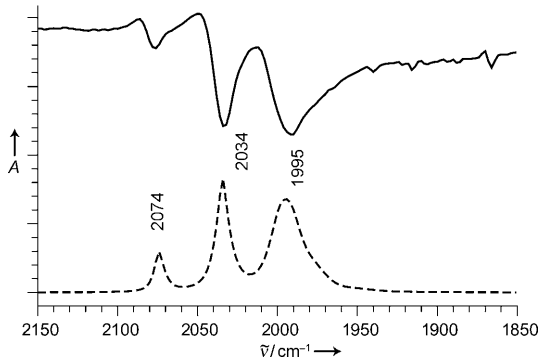

Figure 3. FTIR spectra of the carbonyl stretching region of the $[Fe_2S_2(CO)_6]$ subsite in solution (-----) and bound to the InP nanoparticle film (——). The inversion of the spectrum is indicative of CO bound to conducting nanoparticles.[11,12]

subsite. The "inversion" of the spectrum is a consequence of a surface-enhanced phenomenon associated with the IR-active molecule bound to conducting nanoparticles.[11,12] There is some broadening of bandwidth but a minimal shift in the carbonyl absorption frequencies, thus suggesting the subsite analogue is weakly chemisorbed within the array.

Figure 4 shows the photocurrent obtained at an InP assembly (ten layers) containing the $[Fe_2S_2(CO)_6]$ electrocatalyst upon illumination in 0.1 M aqueous $NaBF_4$ at pH 7 at −400 mV versus {Ag | AgCl, 3 M [NaCl]}. Figure 5 shows the photocurrent obtained at various bias potentials for the InP catalyst electrode array and for appropriate controls. These values make it clear that a significant photoelectrocatalytic current is only observed with the complete InP catalyst assembly. Of note, the maximum photocurrent occurs at a potential more than +250 mV more positive than the H_2/H^+ couple at pH 7. The photocurrent observed at the blank gold electrode and the InP array can be attributed to the well-documented photoelectric effect.[13] The background cathodic dark current is most likely caused by reduction of oxygen traces in the electrolyte.

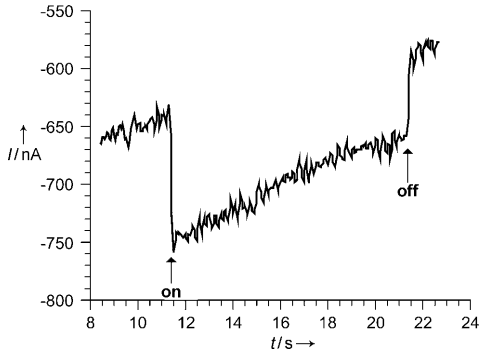

Figure 4. Photocurrent measured at a bias potential of −400 mV versus Ag | AgCl in 0.1 M $NaBF_4$ under illumination with a 395 nm LED. Electrode area: 0.4 cm^2.

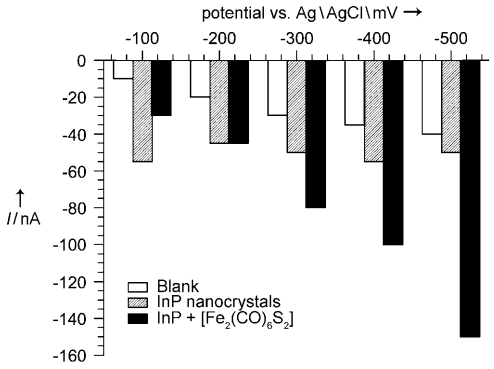

Figure 5. Photocurrent response at different bias potentials. Electrode area: 0.4 cm^2.

A photocurrent could be sustained for at least one hour without degradation at a bias potential of −400 mV (in practice, a slight enhancement of I was observed at longer times), thereby demonstrating the robustness of the system. We used a closed cell, as depicted in Figure 6, for the bulk electrolysis, which allowed us to analyze the gas headspace by gas chromatography. The right hand side of Figure 6 shows the energy diagram of the photocathode and the suggested mechanism for the photocatalytic reduction of protons. After the passage of 2.58 μC (±10%) of charge, we detected a substantial quantity of 16.2 nanomoles of H_2 in the headspace above the electrolyte by gas-chromatography, which corresponds to a current yield of approximately 60%. Control experiments did not show any production of hydrogen.

The mechanism of the H_2 photoproduction probably involves the absorption of incident light by the InP nanocrystals and excitation of an electron into the conducting band of the nanoparticles. Subsequently, electrons are transferred from the conduction band, which lies at about −1.0 V versus Ag | AgCl,[14] into the LUMO of the catalytic subsite at circa −0.90 V versus Ag | AgCl, thereby effecting the reduction of protons. The intimate mechanism of the electrocatalytic hydrogen is likely to involve Fe−H and/or S−H intermediates.[15,16] The holes generated in the valence band of the nanocrystals are immediately filled by electrons available from the underlying gold substrate held at −400 mV versus

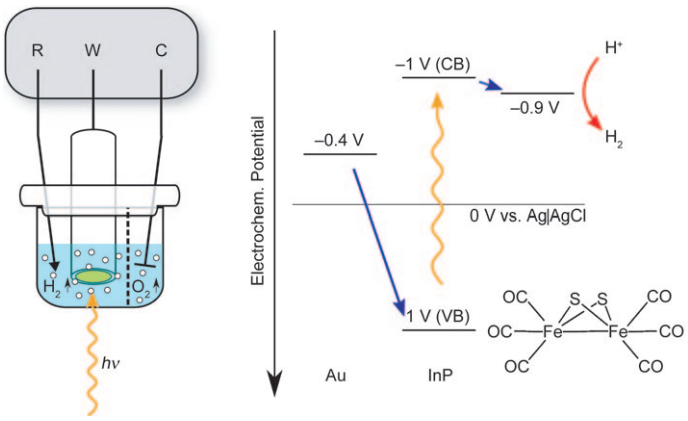

Figure 6. Closed electrochemical cell used (left; R = reference electrode, W = working electrode, C = counter electrode) and energy levels (right; redox potentials of the components of the photocathode; potentials are given versus Ag | AgCl, 3 M NaCl. CB = conduction band, VB = valence band.

Ag | AgCl. The mechanism is depicted on the right hand side of Figure 6.

In conclusion, we have discovered a robust and efficient system for the photoelectrochemical production of hydrogen. The system does not rely on excited states of organic molecules/ligands, unlike most of state-of-the-art approaches. The whole system comprises inexpensive and non-toxic elements, and may be a promising alternative for the inexpensive production of hydrogen.

Experimental Section

Electrochemical measurements were carried out using a HEKA Electronics (Germany) potentiostat type PG 310, and photoelectrochemical experiments were carried out in an aqueous 0.1M $NaBF_4$ electrolyte under dinitrogen in a two-compartment cell at ambient temperature. The platinum secondary electrode was separated from the main compartment of the cell by a frit, so that oxygen produced there did not intermingle with hydrogen produced at the working electrode. Working electrodes were prepared by vapor deposition of gold onto glass slides to a thickness of 200 nm. These were thoroughly rinsed with ethanol and dried.

The photoluminescence of the quantum dots was recorded on a FluoroLog 3 spectrometer from Horiba Jobin (UK). Irradiation was performed using a home-built high-power light-emitting diode array. Reflectance FTIR spectra were recorded on a Perkin–Elmer BX single-beam spectrometer using gold disc electrodes modified with the indium phosphide catalyst array. Hydrogen was measured by gas chromatography using a Hewlett Packard 5890 series II GC with a thermal conductivity detector (TCD) and employing a molecular sieve 5 A (80–100 mesh) 2 m column run at 60 °C with argon as the carrier gas.

Gold electrode modification: All operations were performed under anaerobic conditions (M Braun Lab Star Glove Box, 0.01 ppm O_2), using freshly distilled, degassed solvent. First, the electrode was primed by adsorbing a monolayer of dithiol as a linker, which was achieved by placing 1,4 benzenedithiol (10 μl, 1 mM) in toluene onto the surface of the electrode. After complete evaporation of the thiol solution, the electrode surface was thoroughly rinsed with toluene. An InP nanocrystal solution (10 μl) was then placed onto the electrode, and following the evaporation of the solvent, was again rinsed with toluene. This process was repeated a further nine times to build up a nanoparticle electrode assembly of ten layers. Finally, $[Fe_2S_2(CO)_6]$ was incorporated into the structure by soaking overnight in a 3 mM toluene solution of the complex, followed by thorough rinsing with toluene.

Electrolysis was performed in a closed photoelectrochemical cell operating with a three-electrode configuration. Platinum gauze was used as the secondary electrode (separated from the main compartment by a frit) and Ag | AgCl, 3 M NaCl as the reference electrode (Figure 6, left). The cell was flushed with dinitrogen prior to use and charged with 0.1M aqueous $NaBF_4$ electrolyte. The modified gold photocathode (0.4 cm^2) was placed alongside the secondary and reference electrodes in the cell. The photocathode was illuminated at 395 nm using a light-emitting diode array for 60 min at a constant potential of −400 mV versus Ag | AgCl while the solution was stirred at moderate speed. The gas headspace above the electrolyte was sampled using a gas-tight syringe and analyzed by gas chromatography.

Received: November 6, 2009
Published online: February 5, 2010

Keywords: catalysis · electrochemistry · nanoparticles · quantum dots · water splitting

[1] A. J. Bard, M. A. Fox, *Acc. Chem. Res.* **1995**, *28*, 141 – 145.
[2] A. Fihri, V. Artero, M. Razavet, C. Baffert, W. Leibl, M. Fontecave, *Angew. Chem.* **2008**, *120*, 574 – 577; *Angew. Chem. Int. Ed.* **2008**, *47*, 564 – 567.
[3] Y. Na, M. Wang, J. Pan, P. Zhang, B. Åkermark, L. Sun, *Inorg. Chem.* **2008**, *47*, 2805 – 2810.
[4] E. Reisner, J. C. Fontecilla-Camps, F. A. Armstrong, *Chem. Commun.* **2009**, 550 – 552.
[5] Z. J. Fuller, W. D. Bare, K. A. Kneas, W. Xu, J. N. Demas, B. A. DeGraff, *Anal. Chem.* **2003**, *75*, 2670 – 2677.
[6] A. A. Gorman, M. A. J. Rodgers, *Chem. Soc. Rev.* **1981**, *10*, 205 – 231.
[7] C. Tard, C. J. Pickett, *Chem. Rev.* **2009**, *109*, 2245 – 2274.
[8] F. Gloaguen, T. B. Rauchfuss, *Chem. Soc. Rev.* **2009**, *38*, 100 – 108.
[9] S. Xu, S. Kumar, T. Nann, *J. Am. Chem. Soc.* **2006**, *128*, 1054 – 1055.
[10] S. Xu, J. Ziegler, T. Nann, *J. Mater. Chem.* **2008**, *18*, 2653 – 2656.
[11] Q. Chen, S. Sun, J. Yan, J. Li, Z. Zhou, *Langmuir* **2006**, *22*, 10575 – 10583.
[12] X. Zhou, Q. Chen, Z. Zhou, S. Sun, *J. Nanosci. Nanotechnol.* **2009**, *9*, 2392 – 2397.
[13] G. Y. Kolbasov, V. S. Kublanovskii, T. A. Taranets, K. I. Litovchenko, *Russ. J. Electrochem.* **2002**, *38*, 651 – 654.
[14] S. Kumar, R. Thomann, T. Nann, *J. Mater. Res.* **2006**, *21*, 543 – 546.
[15] T. D. Weatherill, T. B. Rauchfuss, R. A. Scott, *Inorg. Chem.* **1986**, *25*, 1466 – 1472.
[16] C. Tard, X. Liu, S. K. Ibrahim, M. Bruschi, L. D. Gioia, S. C. Davies, X. Yang, L. Wang, G. Sawers, C. J. Pickett, *Nature* **2005**, *433*, 610 – 613.